

KNOT THEORY: CLOSE AND SHARP BOUNDS ON THE GRID INDEX

DIVESH OTWANI

ABSTRACT. In this thesis, we study a knot invariant called the grid index. Knot invariants are functions that take the same value on equivalent representations of the same knot. Heuristically, we find two categories of knot invariants: *semantic* and *computable*. Semantic knot invariants directly represent an interesting property of knots but are in practice hard to compute. On the opposite end, we have a terminating algorithm to find computable invariants but they do not a priori represent a knot property. Here, we study the *grid index* — a semantic knot invariant whose codomain is the naturals — by giving it lower bounds using computable knot invariants, based on the HOMFLY and Dubrovnik knot polynomials.

ACKNOWLEDGEMENTS

“There is only one thing that I dread: not to be worthy of my sufferings.”

— Fyodor Dostoevsky

First and foremost, I am grateful to God. My life and my work is not my own; it is by your grace. To both my parents: thank you for your sacrifice. Dad: it is because of your labor and concern that I have been able to have the life I have. Mom: it is through your nurturing and cooking that I have understood what it means to have a home. To my advisor Professor Josh Sabloff: thank you for your wisdom, guidance and especially your patience. Lastly, to Charles Ashton (my calculus teacher from high school): thank you for seeing something in me and helping me see something in myself.

1. INTRODUCTION

The topic of this thesis is knot theory. Within knot theory, this thesis studies knot invariants: functions such that (1) their domain is some set of *representations* of all knots and (2) these functions take the same value

Date: May 3, 2019.

This document is a senior thesis submitted to the Mathematics and Statistics Department of Haverford College in partial fulfillment of the requirements for a major in Mathematics.

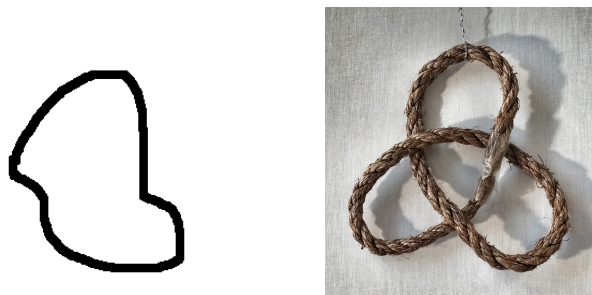


FIGURE 1. The unknot (left) and the trefoil (right) from [9].

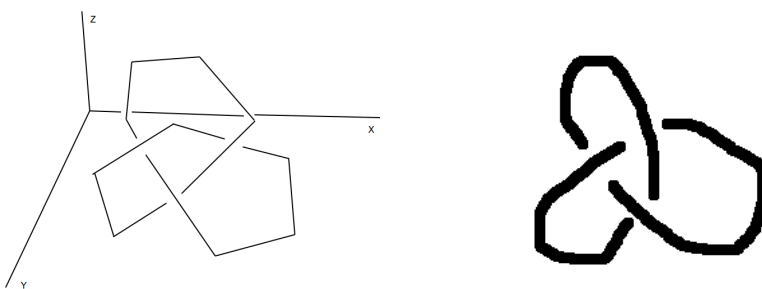


FIGURE 2. Line segment and diagram representations of the trefoil.

over any two representations of the same knot. This overview discusses the representations of knots, which knot invariants we study, and why this work is valuable.

We have two representations of our intuitive idea of a knot. Our pre-mathematical idea of a knot is a piece of string whose ends are glued together. The knot could be a simple loop, also called the *unknot* depicted on the left in Figure 1. Or, of course, the knot could be complicated like the *trefoil*, depicted on the right in Figure 1.

In knot theory, we formalize our intuition with two representations of knots. First, we represent knots as a sequence of line segments in \mathbb{R}^3 . Then, we represent knots with a diagram. Basically, a diagram is a collection of curves in \mathbb{R}^2 which visually look like a string whose ends are glued together by having parts of the string “cross over or under” other parts at places called crossings. For example, we have a line segment and diagram representation of the trefoil in Figure 2.

Of course, there are multiple representations of the same knot. Intuitively, we could move some of the line segments around in the first representation and still be talking about the same knot made out of string. The same

point applies to diagrams. In general, we abstract knots by creating a set of representations of all knots, S , and an equivalence relation \sim over that set.

Once we have a way to represent knots and a definition of which representations yield the same knot, knot invariants become a natural way to (1) study properties of knots and (2) try to tell if two representations are not equivalent. Knot invariants are functions over our set of representations S that have the same value for any two equivalent representations, i.e., any two representations of the same knot. Hence we can test for distinctness: if we have two diagrams D_1, D_2 and a knot invariant f such that $f(D_1) \neq f(D_2)$, then we know $D_1 \not\sim D_2$. Note that the converse does not necessarily hold.

Heuristically, there are two kinds of knot invariants, computable and semantic, and our goal is to place a lower bound on a particular semantic knot invariant with computable knot invariants. Computable knot invariants are those that can be readily computed by looking at one diagram. Specifically, we call a knot invariant computable if we know of a terminating algorithm whose input is a single diagram that computes the value of the knot invariant. On the other hand, semantic knot invariants are not computable, but have the added benefit that they represent some interesting property of knots. For example, for diagram D , let $c(D)$ be the number of crossings on that diagram. There is a knot invariant, called the crossing number, defined as

$$f(D) = \min\{c(D') : D' \sim D\}.$$

While this gives a good idea of how “simple” a knot is (by looking at the minimum number of crossings needed to represent it), it is difficult to compute. (We do not know of an algorithm that can compute this by only looking at one diagram of a knot.) For any diagram we find that is equivalent to the given diagram D , we have an upper bound for the crossing number of D . So, if we could find a lower bound with a computable knot invariant, we have a strategy for finding the crossing number: find a diagram D_c with a crossing number that meets the lower bound, or is close enough that we can rule out the other possible values of the crossing number. *This is the idea behind finding computable lower bounds.*

In this thesis we study the grid index, a semantic knot invariant whose codomain is the natural numbers. We start with some foundational definitions in Section 2. Then, we place two lower bounds on this semantic knot invariant using two computable knot invariants. Our computable knot invariants are polynomial invariants, i.e., their codomain is a ring of polynomials. Finally, we show that for one class of knots, one of our lower bounds is sharp, i.e., our lower bound is the value of the knot invariant.

We state and give an overview of our key theorems.

In Section 3, we give a lower bound of the grid index $\gamma(D)$ via another semantic knot invariant called the braid index $\beta(D)$. This suffices because there exists a polynomial, computable lower bound for the braid index.

Theorem 1.1 (Cromwell [3]). *For any regular diagram D ,*

$$2\beta(D) \leq \gamma(D).$$

In Section 4, we directly use a computable knot invariant. Specifically, we use a computable knot invariant based off of the Dubrovnik polynomial $\mathfrak{D}_D(v, z)$ of a regular diagram D . We use the notation $[\mathfrak{D}_D(v, z)]_v$ to represent the breath of v , i.e., the difference between the highest and lowest powers of v when the polynomial is written in sum of monomials form. This gives us a lower bound on the grid index.

Theorem 1.2 (Morton-Beltrami [6]). *Let D be a diagram with grid index $\gamma(D)$. Then*

$$[\mathfrak{D}_D(v, z)]_v + 2 \leq \gamma(D).$$

In Section 5, we show our second lower bound is sharp for one class of knots: twist knots. This result is our own work.

Theorem 1.3. *Let T_n be a diagram of a twist knot (with $n \geq 0$). Then,*

$$[\mathcal{D}(T_n)]_v + 2 = \gamma(T_n).$$

2. BACKGROUND

2.1. Representations of Knots. Before we can place a computable lower bound on the grid index, we need to understand how to represent knots. First, we create a direct representation with line segments in \mathbb{R}^3 and a standard notion of equality; this representation corresponds closely with our pre-mathematical idea of knots. Then, we build off of this representation and define a “diagram of a line-segment-representation” with an equivalence relation over diagrams. This second representation is more removed from our intuitive idea of a knot but easier to work with. Finally, we state the theorem that says our notion of equality in both representations is the same.

2.1.1. A Line Segment Representation. We begin with a three dimensional representation and the equivalence relation over this representation. The material in this section is a reworking of material from Chapter 1 of [7] and the early chapters of [1].

Definition 2.1. A **polygonal curve** with endpoints $A \in \mathbb{R}^n$ and $B \in \mathbb{R}^n$ is a finite sequence of line segments $P = (l_1, \dots, l_k)$ where segment l_i has endpoints x_i, y_i such that

- $x_1 = A$ and $y_n = B$
- $y_i = x_{i+1}$ for $i \in \{1, \dots, k-1\}$
- each l_i intersects at most two other line segments.

A knot is simply any closed polygonal curve. By convention, however, we will assume any two consecutive line segments when extended to lines do not form the same line.

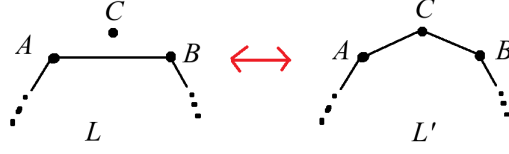


FIGURE 3. The equivalence relation of the line segment representation.

Definition 2.2. A (oriented) **knot** $K = (l_1, \dots, l_k)$ is a polygonal curve with equal endpoints: $x_1 = y_k$. We will write K to mean both the sequence of line segments (l_1, \dots, l_k) and the set of line segments $\{l_1, \dots, l_k\}$. Let $S(K) = \bigcup \{l_1, \dots, l_k\}$, i.e., the set of points that the knot consists of.

The orientation of the knot is the simply the linear order in which K is written. Intuitively, this represents the idea of walking along the string in one direction. We can generalize our definition of a knot to define a link. Links are several knots possibly entwined with each other:

Definition 2.3. A (oriented) **link** L is a finite set of knots $\{K_1, \dots, K_n\}$ such that $S(K_i) \cap S(K_j) = \emptyset$ for any distinct i, j . Let $S(L) = \bigcup S(K_i)$.

We can now present an intuitive notion of which links are equivalent. Essentially, as we can with physical knots made of string, we can move around the segments without having them pass through one another.

Definition 2.4. The **equivalence relation of links** \sim is the smallest equivalence relation such that for any link L with some line segment $\overline{AB} \in K_i \in L$ and any point $C \in \mathbb{R}^3$ the following **triangle move property** holds.

- If $C \notin S(L)$ and $\triangle ABC \cap S(L) = \overline{AB}$, then $L \sim L'$ where

$$K'_i = (K_i - \{\overline{AB}\}) \cup \{\overline{AC}, \overline{CB}\}$$

and

$$L' = (L - \{K_i\}) \cup \{K'_i\}.$$

The idea of this definition is captured in Figure 3. The intuitive idea of moving around the string is captured by replacing one line segment with two that pinch the knot outward (or doing the opposite replacement) under the hypothesis that such a move does not have the “string” pass through itself.

One remark is in order. This equivalence relation is a transitive closure of the relation of all links equal by the triangle move property. Hence, if two links are equivalent we can get from one to the other by a sequence of “triangle moves”. We can intuit that this sequence of triangle moves is finite because knots (and links) are made of finitely many line segments.

2.1.2. Diagram Representation. Our second representation presented here fleshes out content from Chapters one and four of [7].

First, recall the idea of projecting onto a plane in \mathbb{R}^3 :

Definition 2.5. Let P be a plane in \mathbb{R}^3 and v be some vector not on that plane. Recall that each point $x \in \mathbb{R}^3$ can be uniquely represented as $x = kv + p_x$ for some point $p_x \in P$. We define the **projection function on P by v** , denoted $\pi_{P,v} : \mathbb{R}^3 \rightarrow \mathbb{R}^2$, to send

$$x \mapsto [p_x]$$

where $[p_x] \in \mathbb{R}^2$ is the representation of p_x via a fixed orthogonal basis.

We can use projections to create a rough diagram of a link:

Definition 2.6. Let L be a link. A **rough diagram of L on P by v** is the set $\pi_{P,v}[S(L)]$ satisfying the following conditions with suitable P, v :

- (1) $\pi_{P,v}$ is injective on $S(L)$ except for finitely many points, (**finitely many intersections**)
- (2) for all $a \in \pi_{P,v}[S(L)]$, $|\pi_{P,v}^{-1}(a)| \leq 2$, (**no triple points**)
- (3) for all $a \in \pi_{P,v}[S(L)]$ such that $\pi_{P,v}^{-1}(a) = \{x, y\}$ (with $x \neq y$), x and y are not endpoints of any of the line segments in $\cup L$. (**no tangent intersections**)

A few remarks are in order. The projection of any line segment in \mathbb{R}^3 onto a plane becomes a line segment on that plane — though it might be trivial: a line segment parallel to v projects onto a point. In our case, the projection involved in a rough diagram has no trivial line segments. Hence, the ordering of the line segments in the link L translates to the order of the line segments on D . That is, the orientation of the knot is preserved. This definition ensures that our projection has finitely many intersections, none of which are tangent or triple points.

We can change rough diagrams into diagrams like the one in Figure 2:

Definition 2.7. Let L be a link and R be a rough diagram of L with plane P and vector v not on P .

- Suppose we have an intersection at some point $x \in R$. That is, suppose $\pi_{P,v}^{-1}[\{x\}] = \{a, b\}$ with $a \in l$, $b \in l'$ for two distinct line segments: $l, l' \in \cup L$ such that $l \neq l'$. Say a has a farther v -distance from P than b : if $a = p_a + kv$ and $b = p_b + k'v$ for some $p_a, p_b \in P$, then $k > k'$. We form a **crossing** on a rough diagram by taking such an intersection and removing the projection of l' in R inside some open ball $B \subseteq \mathbb{R}^2$ such that B only “captures” that intersection, i.e., $B \cap R \subseteq \pi_{P,v}[l \cup l']$.
- A **regular diagram** is one in which all intersections are replaced by crossings.

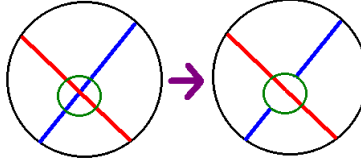


FIGURE 4. Replacing an intersection on a rough diagram with a crossing inside the green open ball.

The idea of creating a crossing from an intersection in a rough diagram is represented in Figure 4. The black circles isolate a single intersection in a larger rough diagram. The blue line segment by v is farther away from the projected plane than the red line segment. Hence, the intersection of that line segment and the green open ball is removed on the right. Note that the open ball is not part of the set of points in the rough (or regular) diagram, but is depicted for clarity.

We note that we can always determine unambiguously the rough diagram from which a regular diagram was made: we simply fill in all the missing line segments at crossings. Hence, given a regular diagram we can assume we have the rough diagram from which we formed this regular diagram. Of course, for one rough diagram there are many regular diagrams (depending on the choice of open balls and which line segments go over or under in crossings).

Now, of course, our new representation needs to be powerful enough to represent all links:

Theorem 2.8 (Adapted from Proposition 1.12 [2]). *Let L be a link. There exists a rough diagram R of L and hence a regular diagram D of L .*

A few remarks are in order. First, for visual appeal, we will draw regular diagrams with smooth curves instead of polygonal curves without modifying the underlying definition. Second, in general, we will treat diagrams combinatorially though underneath the surface, we are really manipulating polygonal curves. Third, we can state our new set of representations of all links:

Definition 2.9. We write \mathcal{D} for the set of all regular diagrams.

Again, we need a notion of which two representations are equivalent.

Definition 2.10. The **equivalence relation \sim of regular diagrams** is the smallest equivalence relation such that the following hold.

- For any line segment \overline{AB} in D with $C \in \mathbb{R}^2$ such that $\triangle ABC \cap D = \overline{AB}$, for $D' = D - \overline{AB} \cup \overline{AC}, \overline{CB}$ we have $D \sim D'$.
- Diagrams changed by **Reidemeister moves**, shown in Figure 5, are equivalent.

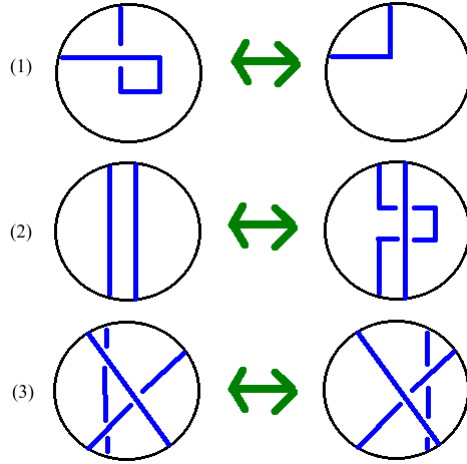


FIGURE 5. The Reidemeister moves on regular diagrams.



FIGURE 6. An example of applying Reidemeister moves.

Note that the second and third Reidemeister moves R_2, R_3 had one strand¹ go under a few other strands but the case where that strands goes over is also called a R_2, R_3 move respectively.

In Figure 6 we apply the second and first Reidemeister moves to show the knot on the left is equivalent to the unknot. In general, two diagram are equivalent if we have some finite sequence of Reidemeister moves and “regular isotopy” moves (moving around a strand without interacting with any crossings or other strands) that get us from one to the other.

Our diagram representation agrees with the “correct” idea of equality that we defined for our first, primitive representation:

Theorem 2.11 (Theorem 4.1.1 [7]). *Let L, L' be links and D, D' be diagrams of those links respectively. Then,*

$$L \sim L' \text{ if and only if } D \sim D'.$$

¹We use this term to refer to a few consecutive line segments of a knot.

2.1.3. *Knot Invariants.* We can study knots by studying our formalized representation. A primary way we do this is through knot invariants:

Definition 2.12. Let S be a set and \sim be an equivalence relation over S . Let $f : S \rightarrow T$ be some function. We say f is a \sim invariant if for all $a, b \in S$, $a \sim b$ implies $f(a) = f(b)$. If $S = \mathcal{D}$, then f is a **knot invariant**.

In this thesis, we interact with the grid index, the braid index and the Dubrovnik polynomial knot invariants. The codomain of the first two are natural numbers while the codomain of the last is a Laurent polynomial, a polynomial in $\mathbb{Z}[v^{\pm 1}, z^{\pm 1}]$. Since knot invariants f are invariant on any regular diagram D of a link L , we may write $f(L)$ to represent the value of the invariant on any diagram of L . Usually, we write $f(D)$.

2.2. **Grids.** The grid index is a knot invariant that represents how combinatorially simple a knot is. We will see that we can always find a diagram for a knot in a combinatorial form that we call a grid form and that this enables us to define an invariant for the most simple grid-form diagram we can find for a knot. Our work here restructures and simplifies the definitions and ideas from [5] and [8]. The proof ensuring the grid form exists for any knot is non-traditional and original.

Definition 2.13. Let D be a regular diagram of rough diagram R . Write $R = \cup\{l_1, \dots, l_k\}$ for line segments l_i . We say D is in **grid form** with **grid number** n , denoted $g(D)$, if there is a n by n grid such that the following are satisfied.

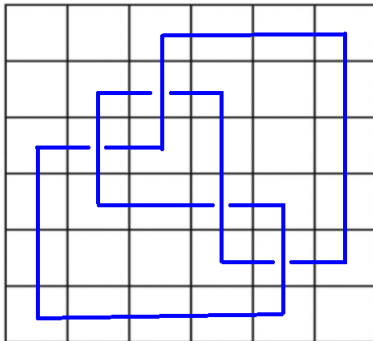
- (1) Each l_i is either vertical or horizontal.
- (2) Each column and row of the grid has exactly one vertical and horizontal line segment.
- (3) Note that each intersection on R is between a vertical and horizontal line segment because of the last two conditions. For each intersection $x \in R$ between a horizontal line segment l_h and a vertical line segment l_v , the intersection of l_h and some open ball containing $x \in R$ is missing in D .²

Definition 2.14. Let L be a link with regular diagram D . Define $\mathcal{G}(D)$ to be the set of diagrams equivalent to D in grid form.

See Figure 7 for an example. We can always find a grid-form diagram for a link:

Theorem 2.15. *Let D be a regular diagram. Then $\mathcal{G}(D)$ is non-empty.*

²That is, for any intersection in the rough diagram, a piece of the horizontal line segment around the intersection is removed in the regular diagram.



To prove Theorem 2.15 we need two lemmas and a few definitions. Our proof centers around getting a sparse and orthogonal diagram.

- A vertical line segment at x_0
- An endpoint of two non-vertical line segments with x value x_0
- An intersection in R with x value x_0

Definition 2.17. A regular diagram D with rough diagram R is **orthogonal** if all line segments of R are horizontal or vertical.

Lemma 2.18. *Let D be a regular diagram. There is an equivalent regular diagram D' that is sparse and preserves the orthogonality of D and the orientation of each orthogonal crossing (i.e., whether the vertical line segment goes over or under).*

For all non-vertically connected endpoints and intersections at x_0 , pick some open square around that endpoint or intersection only containing that endpoint or intersection. That is, if line segments l, l' form the endpoint or

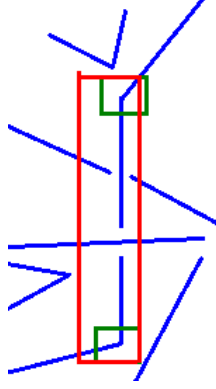
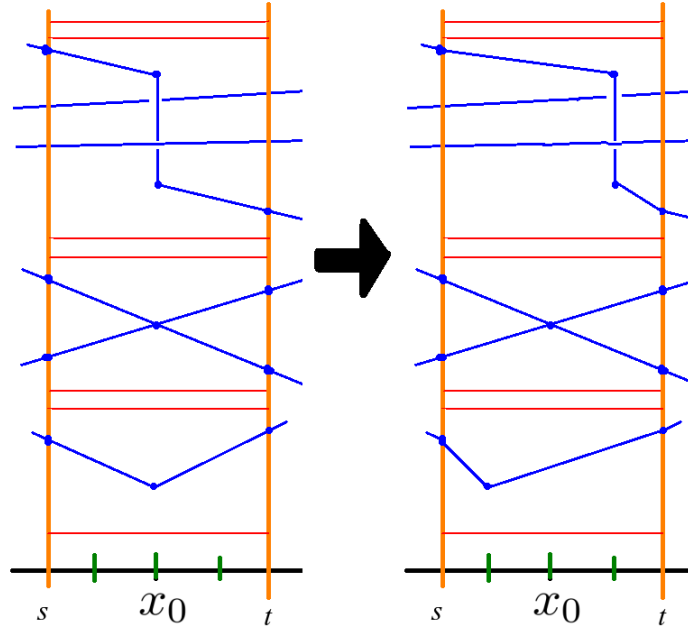


FIGURE 8. Picking an open rectangle on a vertical line segment.


 FIGURE 9. Regular isotopies on a non-simple x value.

intersection in R and S is the open square, $S \cap R \subseteq (l \cup l')$. Call the set of these open squares A .

For each vertical line segment v at x_0 , pick an open square around the top and bottom endpoints. Let a, b be the height of the top square and the depth of the bottom square respectively. As in Figure 8, take some open range (p, q) such that $p < x_0 < q$ and the only line segments in the rectangle

defined by $[a, p, b, q]$ are v , the two line segments at the endpoints of v and all line segments that intersect v .

Find the minimum and maximum x values of the open rectangles in $A \cup B$ and let that form an open range (s, t) such that $s < x_0 < t$ as in Figure 9. The red lines are the tops and bottoms of the original open rectangles in $A \cup B$. Note that all points except for x_0 in (s, t) are very simple. Let k be the number of endpoints, intersections and vertical segments. Mark k distinct endpoints (shown in green) along (s, t) and perform the regular isotopy moves shown in the figure moving each endpoint, intersection and vertical line segment to a distinct mark.

It is easy to see that the bottom two changes in our figure are regular isotopies. For the third change, since no intersections (aside from those at x_0) exist inside the range (s, t) we can view the strand of the vertical line segment as being at some distinct height and all the intersecting line segments moving under or over. Hence, that regular isotopy simply moves the strand at its own height.

Therefore, our resulting diagram D' is equivalent to D . Since our k marks were at very simple values, we have reduced the number of non-simple x values by one. Note that we have not changed the y -value of any endpoint or crossing. Further, we have not introduced any new horizontal line segments. So, we have not changed the number of non-simple y values. By our inductive hypothesis, this suffices to ensure an equivalent sparse diagram.

Finally, we need to show we preserve orthogonality and the orientation of orthogonal crossings. Our move does not introduce any non-orthogonal line segments. Hence, we need only consider whether we change any orthogonal line segments to not be orthogonal. Inspect our three cases in Figure 9. In the bottom and top cases, if one of our line segments leaving the range is horizontal, since we do not change the height of the endpoint at x_0 (or the endpoints in the top case), it will still be horizontal at the end of our move. The intersection cannot have any orthogonal line segments and our change cannot add one. Hence, D' is orthogonal if D was orthogonal. Now, if there is a orthogonal intersection, it must appear in the top case in our figure. We may observe that whichever strand goes over is preserved. \square

Lemma 2.19. *Suppose D is an orthogonal sparse regular diagram with rough diagram R . There is some square grid G such that each row (column) of G contains exactly one horizontal (vertical) line segment of R .*

Proof. Let V, H be the set of vertical and horizontal line segments of R . Note that $|V| = |H|$. If we assign an orientation to D we can construct a bijection $f : V \rightarrow H$ that takes each vertical line v segment to the horizontal line segment h that connects to the endpoint e of v in the direction of the orientation. See Figure 10.

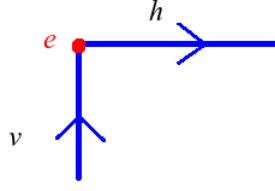


FIGURE 10. The bijection between vertical and horizontal line segments f ; here $f(v) = h$.

Since (by sparseness) no line segments of V or H share x or y values respectively, write the occupied x or y values of the line segments of V, H as $X = \{x_1, \dots, x_n\}$, $Y = \{y_1, \dots, y_n\}$ such that $x_i < x_{i+1}$ and $y_i < y_{i+1}$. Select $(n+1)$ x and y values $A = \{a_1, \dots, a_{n+1}\}$ and $B = \{b_1, \dots, b_{n+1}\}$ such that

$$a_i < x_i < a_{i+1}, \quad b_i < y_i < b_{i+1}.$$

Then, the grid G formed by the union of all horizontal and vertical line segments with x values in A and y values in B is what we desire. Any column of the grid has x values (a_i, a_{i+1}) for some i . By design, there is exactly one vertical line segment in that column, the one with x value x_i . A similar argument works for rows. Since $|A| = |B| = n+1$, the grid is square. \square

Using these lemmas, we prove Theorem 2.15.

Proof of Theorem 2.15. Let D be a regular diagram with rough diagram R . We make the following changes to D .

- (1) We take each line segment l that is non-orthogonal and apply one of the two forms of the mountain-valley move in Figure 11: between the crossings on the line segments, pick some point (shown in black) whose x value is very simple. We may do this since we have infinitely many points and finitely many non-simple values.

We alternate, going left to right, in moving pieces up (as mountains) and down as valleys as shown. If the left endpoint connects to a downward vertical line segment we start with a mountain (and an upward vertical line segment makes us start with a valley).

Each piece has one crossing. If the intersecting strand crosses over l , we push our mountain or valley below all other parts of D (and vice versa) via R_2, R_3 moves. As we do this, we ensure that the height of each new mountain is above all other parts of the diagram (and similarly for valleys). This way, all horizontal line segments we introduce have no intersections. Finally, if we find that we cannot make a mountain or valley for the last piece of the line segment because the segment connecting to the right endpoint is vertical, we simply choose

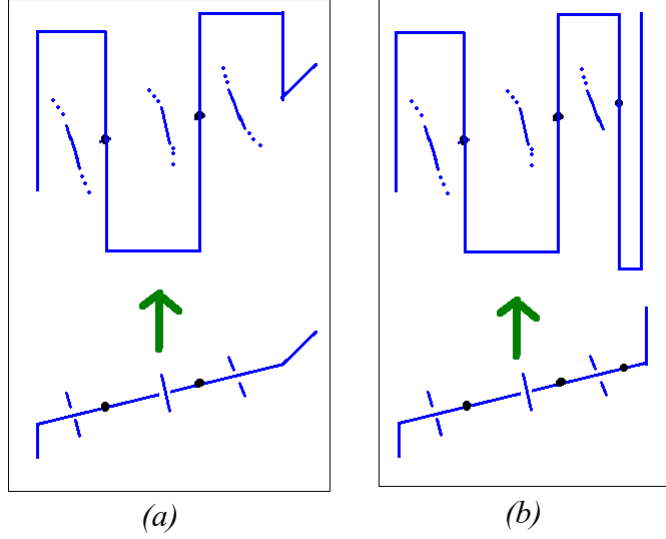


FIGURE 11. Two versions of the **mountain-valley move** on a non-orthogonal line segment.

another very simple point as in version (b) and add a mountain or valley.

Since we chose very simple points on which to add vertical line segments (or just extended existing vertical line segments), we have not introduced any triple points or tangent intersections. Also, recall that our horizontal line segments have no intersections by construction. Hence, our result is an orthogonal regular diagram.

- (2) Since the diagram is orthogonal, any crossing is a plus sign. For each crossing in which the vertical strand crosses under the horizontal strand, using some open square capturing only that crossing, make a twist move as in Figure 12.
- (3) We still have a diagram which is orthogonal. By Lemma 2.18, we make our diagram both orthogonal and sparse while preserving the orientation we set for each crossing in the previous step.

By Lemma 2.19, there exists a grid where each row and column contains exactly one line segment. Our crossings are in the desired orientation and hence we have an equivalent grid diagram. \square

After this long technical result, we can define the grid index:

Definition 2.20. Let D be a regular diagram. Recall $g(G)$ denotes the grid number of a diagram G in grid form. The **grid index** of D is defined as

$$\gamma(D) = \min\{g(D') : D' \in \mathcal{G}(D)\}.$$

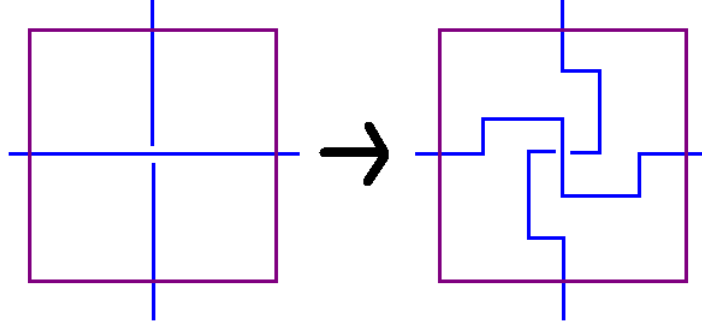


FIGURE 12. A **twist move** on an unsuitable orthogonal crossing.

This is the smallest grid we can squeeze the link represented by D onto. The lower a link's grid index, the simpler it is. Note that this semantic invariant is much more descriptive than the crossing number. Though we will not explore this, some diagrams with minimal crossings are far more complicated than diagrams without minimal crossings. However, this is typically not the case for grid numbers; the grid index seems to represent the minimal amount of information we need to know to unambiguously specify a link.

2.3. Braids. In analogy with grids, in this section we also describe a specific form of a regular diagram and define a natural number, semantic knot invariant based on that form. Specifically, we will define when a diagram is a closure of a braid. Then, we will define an invariant based on the set of diagrams in braid-closure form that are equivalent to a given diagram. This material reformulates content from Chapter 10 of [7] and 5.4 of [1].

Definition 2.21. A **braid closure of degree n** is a diagram D from rough diagram E such that there is some rectangle R bounding the solid region R' satisfying the following. See Figure 13.

- (1) Label two opposite sides of R as s, t . $E \cap R'$ and $E - R'$ consist of n polygonal curves each of which has one endpoint on s and one on t .
- (2) Fix one endpoint of s and call it e and do the same for the opposite endpoint e' on t . Label the points of E on s, t by the distance from e, e' as s_1, \dots, s_n and t_1, \dots, t_n where s_1, t_1 is the closest point of E on s, t to e, e' respectively. Any polygonal curve in $E - R'$ must connect two matching endpoints s_i, t_i for some $i \in \{1, \dots, n\}$.
- (3) For each polygonal curve c with sequence of endpoints e_1, \dots, e_k in $E \cap R'$, with $e_1 \in s$ and $e_k \in t$, the sequence of distances of these points from s , denoted $(d(e_1), \dots, d(e_k))$ is increasing.
- (4) There are no crossings in $D - R'$.

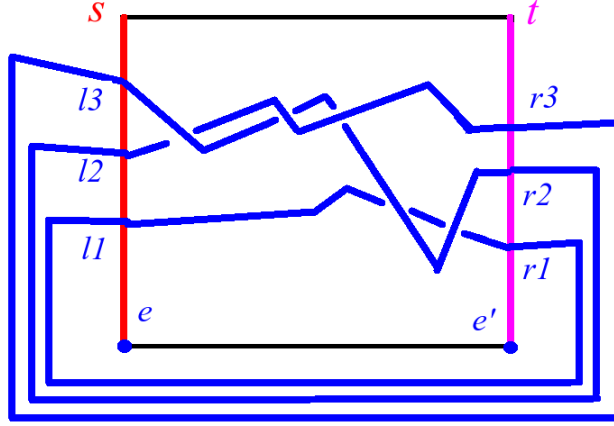


FIGURE 13. A braid closure in the style of Definition 2.21.

We use the terms braid and braid closure interchangeably. Now, following our previous pattern, we show braid closures always exist:

Definition 2.22. Let D be a regular diagram. Then $\mathcal{B}(D)$ is the set of all regular diagrams equivalent to D that are the closures of some braid.

Theorem 2.23 (Alexander's Theorem, [7] 10.3.1). *Let D be a regular diagram. Then, $\mathcal{B}(D)$ is non-empty.*

The proof will follow from Lemma 3.3 and Theorem 2.15. Theorem 2.15 states for any diagram, there exists an equivalent diagram in grid form. In Lemma 3.2, we take a diagram in grid form and construct a braid closure that is equivalent to it. Hence, these two together prove the existence of an equivalent braid closure for any diagram. We remark that this proof is not the classical proof for the existence of an equivalent braid closure for any diagram. (The classical proof is called Alexander's Theorem, discussed in Chapter 10 of [7].)

Now, as before, we can readily define the knot invariant.

Definition 2.24. Let D be a regular diagram. Let $b(D')$ denote the degree of D' , a diagram in braid-closure form. The **braid index** of D is defined as

$$\beta(D) = \min\{b(B) : B \in \mathcal{B}(D)\}.$$

2.4. Cascade Form. Our second lower bound in Section 4 relies on relating diagrams in grid form to diagrams in a specific form called cascade form. The material in this section reformulates definitions in Section 3 of [6].

Definition 2.25. A regular diagram D with rough diagram R is in **cascade form** with **degree** n if there is some simple closed curve F (called a frame) such that the following hold. Let F' be the solid region bounded by F .

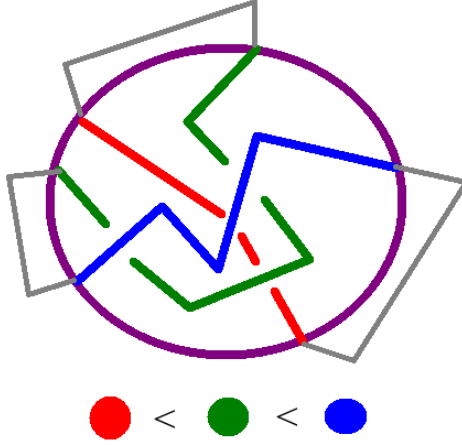


FIGURE 14. An example of a diagram in cascade form.

- (1) $F \cap R$ consists of $2n$ (distinct) points.
- (2) $F' \cap R$ consists of n polygonal curves. (Note: these do not share endpoints and each curve has distinct endpoints.)
- (3) No curve in $F' \cap R$ intersects itself inside $F' \cap R$.
- (4) There are no intersections in $R - F'$.
- (5) Let F^* be the open region bounded by F . Say a polygonal curve $c \subseteq (R - F^*)$ connects two points $e, e' \in F$. Let X be the open region bounded by c and F . Then $X \cap D = \emptyset$. These curves are called **caps**.
- (6) Number the n curves in $F' \cap D$ as c_1, \dots, c_n . There exists a linear order denoted (\prec) on c_i such that for each crossing between c_i, c_j where c_i is the over strand, we have $c_j \prec c_i$.

See Figure 14 for an example. Everything except for the purple is part of the regular diagram. The purple closed curve is the frame F . There are 6 points on $F \cap D$ and three polygonal curves in $F' \cap D$ which connect these points. There is a green, red and blue curve. There are no intersections in $R - F'$. All the grey caps in $D - F^*$ along with F bound empty regions. Finally, as shown there is a linear order on these curves that “agrees with” all crossings.

2.5. The Dubrovnik-Based Polynomial Invariant. Our lower bound in Section 4 is based on a knot invariant formed using the Dubrovnik polynomial. Our definitions and theorems here are from [6].

The Dubrovnik polynomial itself is *not* a knot invariant. However, we are able to use it to define a knot invariant.

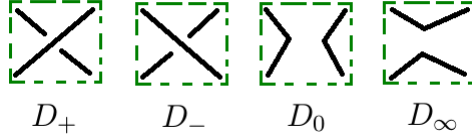


FIGURE 15. Versions of a crossing for the **Dubrovnik skein relation** from [6].

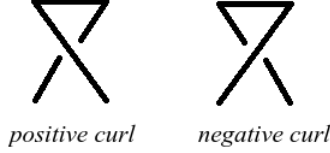


FIGURE 16. Assigning signs to curls.

Theorem 2.26 ([6]).

I. *There is a unique polynomial $\mathfrak{D}_D(v, z)$ for each regular diagram D that satisfies the following. Note: for ease of notation, we sometimes omit the variables v, z and write $\mathfrak{D}(D)$.*

- $\mathfrak{D}(\mathcal{O}) = 1$ where \mathcal{O} is the diagram of the unknot with no crossings.
- The **skein relation** holds:

$$\mathfrak{D}(D_+) - \mathfrak{D}(D_-) = z\mathfrak{D}(D_0) - z\mathfrak{D}(D_\infty)$$

where D_+, D_-, D_0, D_∞ are diagrams which are identical except at one crossing as in Figure 15.

- We have

$$\mathfrak{D}(D^*) = v\mathfrak{D}(D)$$

$$\mathfrak{D}(-D^*) = v^{-1}\mathfrak{D}(D)$$

where D^* adds a negative curl to D and $-D^*$ adds a positive curl to D . Positive and negative curls are depicted in Figure 16.

II. *The polynomial $\mathfrak{D}_D(v, z)$ is invariant under R_2, R_3 moves.*

We implicitly note that we can always compute $\mathfrak{D}(D)$ using the relations above. For conciseness, we will call the Dubrovnik bracket polynomial simply the bracket polynomial. Our lower bound depends on the breadth of the bracket polynomial.

Definition 2.27. Let $p \in \mathbb{Z}[x_1^\pm, \dots, x_n^\pm]$. Write

$$\bar{x} = (x_1, \dots, x_{i-1}, x_{i+1}, \dots, x_n)$$

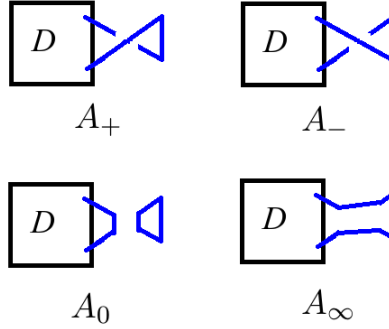


FIGURE 17. Diagrams for a skein relation for Proposition 2.29.

and

$$p(x_1, \dots, x_n) = a_m x_i^m f_m(\bar{x}) + \dots + a_M x_i^M f_M(\bar{x})$$

where a_m, a_M, f_m, f_M are nonzero, m, M are the minimum and maximum powers of x_i and f_i are Laurent polynomials. Then, we say the **breadth of x_i in p** is $(M - m)$ and denote this by $[p]_{x_i}$.

For example, $[xy^2 - z^{-3}y^{-4} - y^3]_y = 3 - (-4) = 7$.

Corollary 2.28. *For all D , $[\mathfrak{D}(D)]_v$ is a knot invariant.*

Proof. If two diagrams D, D' are equivalent there is a finite sequence of Reidemeister moves and regular isotopy moves (x_1, \dots, x_n) that change one into the other. By Theorem 2.26, if x_i is a R_2 or R_3 move the polynomial does not change. The polynomial does not change for a regular isotopy move because such moves can be reversed without adding or removing crossings or curls (keeping the calculation the same). Finally, observe that R_1 moves simply multiply or divide the bracket polynomial of the original diagram by a factor of v which does not change the breadth. \square

In our computations, we will rely on one property of the Dubrovnik bracket:

Proposition 2.29 (From [6]). *Let D be a regular diagram and $D \sqcup \mathcal{O}$ denote a regular diagram that includes D with one disjoint unknot that has no crossings. Then*

$$\mathfrak{D}(D \sqcup \mathcal{O}) = \delta \mathfrak{D}(D),$$

where $\delta = 1 + z^{-1}(v^{-1} - v)$.

Proof. We construct a diagram A_+ that is D with an added positive curl at one end as in Figure 17. Consider the skein relation on the crossing of that positive curl. By Theorem 2.26, we can use the behavior of the bracket polynomial on curls to say $\mathfrak{D}(A_+) = v^{-1}\mathfrak{D}(D)$ and $\mathfrak{D}(A_-) = v\mathfrak{D}(D)$. Now,

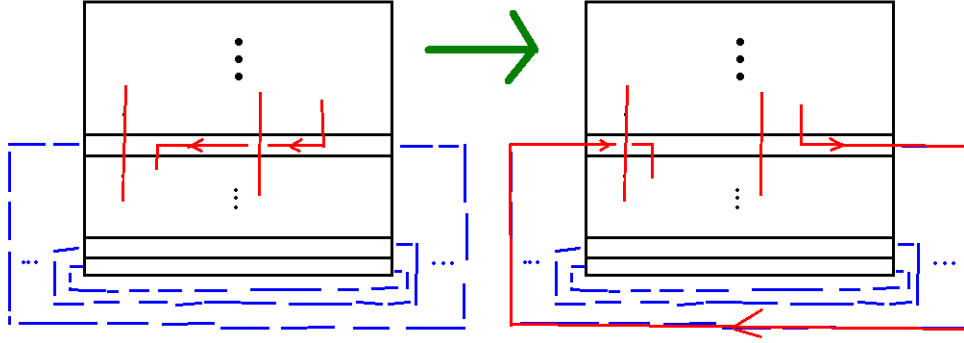


FIGURE 18. A **loop-inversion** move on a grid diagram for row k . The red horizontal strand is moved to follow the dotted blue guide line.

observe that $A_0 = D \sqcup \mathcal{O}$ and $A_\infty = D$. Hence, $\mathfrak{D}(A_0) = \mathfrak{D}(D \sqcup \mathcal{O})$ and $\mathfrak{D}(A_\infty) = \mathfrak{D}(D)$. Using Theorem 2.26 we write the skein relation and solve for A_0 :

$$\begin{aligned} \mathfrak{D}(A_+) - \mathfrak{D}(A_-) &= z\mathfrak{D}(A_0) - z\mathfrak{D}(A_\infty) \\ \mathfrak{D}(A_0) &= z^{-1}(\mathfrak{D}(A_+) - \mathfrak{D}(A_-) + z\mathfrak{D}(A_\infty)) \\ \mathfrak{D}(D \sqcup \mathcal{O}) &= z^{-1}(v^{-1}\mathfrak{D}(D) - v\mathfrak{D}(D) + z\mathfrak{D}(D)) \\ &= (1 + z^{-1}(v^{-1} - v))\mathfrak{D}(D) \end{aligned}$$

□

3. BRAID INDEX LOWER BOUND

With our background in place, we prove Theorem 1.1, our first lower bound of the grid index. As stated before, it suffices to bound the grid index below by the braid index because we already know of a polynomial computable lower bound for the braid index. The results in this section heavily rework results from [3].

We need two lemmas to bound the grid index by the braid index. First, we need to be able to make a certain kind of change to our diagram and still get an equivalent diagram.

Definition 3.1. A **loop-inversion move** on a diagram in grid form for row k is depicted in Figure 18.

Lemma 3.2 (Cromwell [3]). *Let D be a regular diagram and D' be the diagram obtained by doing a loop-inversion move on D . Then, $D \sim D'$.*

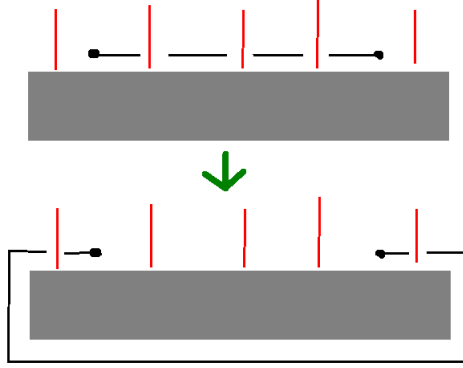


FIGURE 19. A generalized R_2, R_3 move that swings a strand under a rectangle.

Proof. Inspect Figure 19. We do a generalized R_2, R_3 move by essentially swinging the strand in some row of the grid under some solid gray region. The solid region we abstract away is the rectangle formed from the row below and the blue dotted lines leaving that row. \square

This lemma enables our second lemma:

Lemma 3.3 (Cromwell [3]). *Let D be a diagram in grid form with grid number n . For some $m < n$, there are braids equivalent to D of degree m and $n - m$.*

Proof. Let D be a diagram in grid form with grid number n . Mark the orientations of each horizontal line segment. For each of the m line segments whose orientation is right to left, replace it as in Figure 18 to be left to right. By Lemma 3.2, the resulting diagram D' is equivalent to the first. For reference, see the conversion of the trefoil in Figure 20.

Now, we show D' is a braid of degree m . Recall that the rough diagram from which D' comes from is simply one in which all crossings become intersections where the “under-strand” continues in a straight line to the other side. Call this rough diagram X . Call the frame of the grid R and the solid region inside R' . Let l, r be the left and right sides of the square and number the points of $X \cap R$ on l and r from top to bottom as l_1, \dots, l_m and r_1, \dots, r_m . Now, we show D' is a braid using R by checking our four conditions. See Figure 18.

- (1) By construction, there are m curves in $X - R'$. These are the m curves following the blue dotted lines connecting l_i to r_i . Given any left endpoint l_i , the curve starting at l_i inside R must connect to some point r_j . This is because the orientation of line segments is only up,

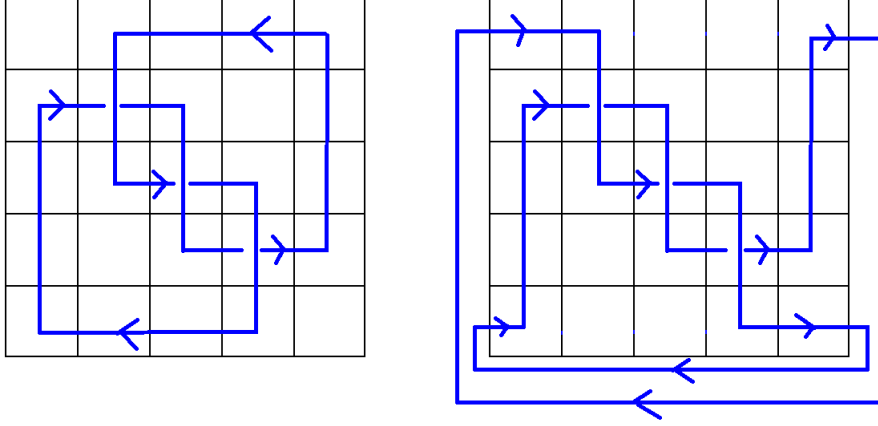


FIGURE 20. A trefoil in grid form (left) and the transformation into a braid (right).

down or right and after each vertical line segment, there must be a rightward line segment. By construction, only one line segment meets each endpoint r_i so there are exactly m curves in $X \cap R'$.

- (2) By construction via our blue dotted lines, the curves in $X - R'$ connect l_i to r_i .
- (3) Let c be a polygonal curve inside $X \cap R'$ from l_i to r_j with endpoints $(l_i = e_1, \dots, e_k = r_j)$. Let $d(e_i)$ be the distance from each endpoint to l . To show the sequence $(d(l_i) = d(e_1), \dots, d(e_k) = d(r_j))$ is increasing it suffices to show that any two consecutive elements are increasing. So, pick two consecutive endpoints e_q, e_{q+1} . Either these form a vertical line segment or a horizontal one. If these form a vertical line segment, it is parallel to l and $d(e_q) = d(e_{q+1})$. In this case, the pair is increasing: $d(e_q) \leq d(e_{q+1})$. If these form a horizontal line segment, it must have a left to right orientation. That is, $\overline{e_q e_{q+1}}$ is a line segment perpendicular to l to the right of l . We must have $d(e_q) < d(e_{q+1})$ as desired.
- (4) By construction, none of the blue dotted line segments intersect. Hence, none of the m curves in $X - R'$ intersect.

Hence, D' is a braid of degree m . Finally, observe that the same process can be applied to change the $n - m$ horizontal strands of D that go from left to right to go from right to left. The result would be a braid of degree $n - m$ equivalent to D . \square

Finally, from here, we can prove Theorem 1.1. That is, we can show for any diagram D , $2\beta(D) \leq \gamma(D)$.

Proof of Theorem 1.1. Let D be a regular diagram. We may assume D is in grid form with grid number $n = \gamma(D)$ by Theorem 2.15. By Lemma 3.3, we have two braids B, B' equivalent to D with one having degree m and one having degree $n - m$ for some $0 < m < n$.

We must have either $m \leq \frac{n}{2}$ or $n - m \leq \frac{n}{2}$. Otherwise, we can add $m > \frac{n}{2}$ and $n - m > \frac{n}{2}$ to get $(n - m) + m = n > n = \frac{n}{2} + \frac{n}{2}$ which is a contradiction. Thus, we must have some braid of degree d such that $d \leq \frac{n}{2} = \frac{\gamma(D)}{2}$. If the braid index of D is $\beta(D)$, then by definition of the braid index, $\beta(D) \leq d \leq \frac{\gamma(D)}{2}$, which implies $2\beta(D) \leq \gamma(D)$. \square

This work is useful because there is a known computable lower bound of the braid index that uses a computable polynomial invariant called the HOMFLY polynomial, $P_D(v, z)$ for regular diagram D .

Theorem 3.4 (Morton-Franks-Williams [4]). *Let D be a regular diagram. We then have the following inequality:*

$$[P_D]_v + 2 \leq 2\beta(D).$$

Using this well-known result above, we easily get a computable lower bound for the grid index:

Corollary 3.5 (Cromwell [3]). *Let D be a regular diagram. Let $[P_D]_v$ be the breadth of the v variable in the HOMFLY polynomial $P_D(v, z)$. We then have the following inequality:*

$$[P_D]_v + 2 \leq \gamma(D).$$

4. DUBROVNIK-BASED LOWER BOUND

Theorem 1.2, our second lower bound, depends on two results from [6] involving diagrams that are in cascade form. After we discuss these in the next two sections, we provided a detailed version of the proof of the bound found in [6].

4.1. Grids to Cascades. In this subsection, we show the first result; we show that we can take a diagram in grid form with grid number n and create an equivalent regular diagram that is a cascade of degree n . We provide a unique proof for this result based off the proof from [6].

Theorem 4.1 (Morton-Beltrami [6]). *Let D be a diagram in grid form with grid number n . Then, there exists a regular diagram D' equivalent to D that is a cascade of degree n .*

Proof. Suppose we have a diagram D in grid form with grid number n . For each left endpoint of each of the n horizontal segments, perform a finger pop as in Figure 21. This finger move is successively using R_2 moves always making the finger go under in any crossing we introduce. Note that each

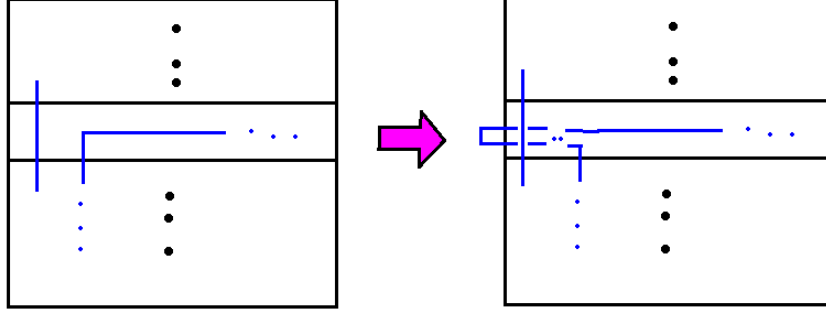
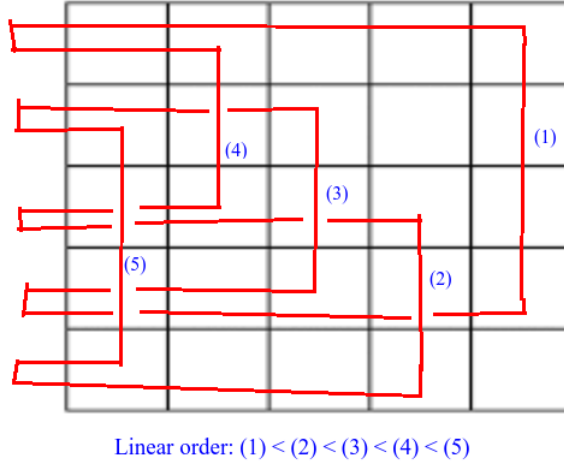
FIGURE 21. A general **finger pop** on a diagram in grid form.

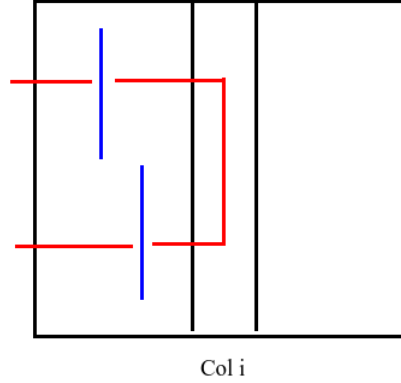
FIGURE 22. A cascade of the trefoil made from a diagram in grid form.

finger stays in the row of the horizontal segment it is identified with. An example of this done on the trefoil is depicted in Figure 22.

Call this resulting equivalent diagram D' . We claim D' is a cascade of degree n where the frame F is the border of the grid. Let F' be the solid region bounded by F .

Number the columns of the grid from *right to left* from 1 to n . Call the curve corresponding to the vertical segment in column i , c_i as in Figure 23.

First, we show each point lies on one of these curves. If P is a point in $F' \cap D$, then either P is on a vertical segment, on a horizontal segment, or it is on one of the introduced fingers. If P is on a vertical segment in column i , it lies on curve c_i . If P is on a horizontal segment, since only the left endpoints of horizontal segments have changed, the right endpoint of that horizontal


 FIGURE 23. The red curve c_i formed by finger-pop moves.

segment connects to some vertical segment with curve c_j . This point must lie on that curve. Finally if P lies on a finger, it can lie on the top or bottom of the finger. Say that finger is in a row with a horizontal segment whose endpoints are in columns i, j with $i < j$ (so c_i is to the right of c_j). If P is on the top of the finger, it connects to c_i and c_j if it lies on the bottom.

Now, order the curves $c_1 < \dots < c_n$. Suppose we have an arbitrary crossing between curves c_i, c_j . Observe from Figure 23 that the only crossings are formed by the horizontal portions of some curve crossing under vertical line segments to the left of that curve. Hence, if c_i crosses under c_j we must have one of the horizontal portions of c_i cross the vertical segment in column j which is to the left of c_i . That is, we must have $i < j$ as desired.

Observe that the curves outside of F' bound empty regions. Since we have n curves inside of $F' \cap D$ with the crossings respecting some linear order, we have a cascade of degree n . \square

4.2. Dubrovnik-Breadth Bounds on Cascades. Our Dubrovnik-breadth-based lower bound requires a second central lemma: we show that given a diagram that is in cascade form of degree n , we have an upper (lower) bound on the highest (lowest) power of v in the Dubrovnik polynomial of that diagram. We provide a detailed exposition of this proof from [6].

Theorem 4.2 (Morton-Beltrami [6]). *Let K be a diagram that is in cascade form of degree d . Write*

$$\mathfrak{D}(K) = a_m v^m P_m(z) + \dots + a_M v^M P_M(z)$$

such that $a_m \neq 0, a_M \neq 0, P_m \neq 0, P_M \neq 0$ and m, M are the minimum and maximum powers of v . Then, $M \leq d - 1$ and $m \geq 1 - d$.

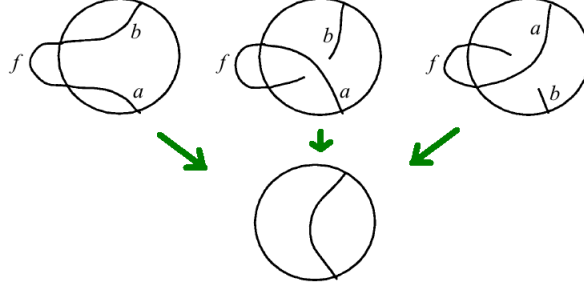


FIGURE 24. A move on adjacent caps in a cascade.

Proof. Let K be a diagram that is a cascade of degree d and write $\mathfrak{D}(K)$ as in the statement of the theorem. We proceed by lexicographic induction on (d, n) where n is the number of crossings of K .

Base case: Let $d = 1$. If the inside of the frame has one curve and no intersections lie outside the curve, our diagram must be the unknot with no crossings. The Dubrovnik polynomial is 1 and $m, M = 0$.

Inductive case: Suppose our result holds for $(d', n') < (d, n)$. Pick some cap f of K with points P, Q on the frame F . Let F' be the solid region inside F . Here, we take cases on f :

- **Case 1:** A single curve c inside $F' \cap K$ joins P, Q . Since f is a cap and nothing is inside the region it forms with F , by regular moves we can say our diagram K is $\mathcal{O} \sqcup K'$ for some diagram K' that is a cascade of degree $d - 1$. By Proposition 2.29 we know

$$\mathfrak{D}(K) = \mathfrak{D}(K')(1 + z^{-1}v^{-1} - v).$$

Say the lowest and highest power of v in $\mathfrak{D}(K')$ are m', M' . From this equation $m = m' - 1$ and $M = M' + 1$. By the inductive hypothesis, $M' \leq (d-1)-1$ and $m \geq 1 - (d-1)$. This implies $M = M' + 1 \leq d - 1$ and $m = m' - 1 \geq 1 - d$ as desired.

- **Case 2:** Suppose that two distinct curves a, b inside $F' \cap D$ meet f . Say the curve a has endpoints P and P' ; say the curve b has endpoints Q and Q' . Without loss of generality, say $a \succ b$ in the linear order of the cascade (\prec) . Suppose that according to (\prec) , there are k curves between b and a . We induct on k in the ordering

$$b \prec x_1 \prec \cdots \prec x_k \prec a.$$

- **Base case:** $k = 0$. Two curves that meet a cap under regular equivalence either have one or no crossings. In any case, we change K to another diagram K' with the replacement from Figure 24. The resulting diagram is a cascade with one fewer

curve (and degree), and hence, our outer inductive hypothesis tells us that if m', M' are the minimum and maximum powers of v in $\mathfrak{D}(K')$, then $M' \leq (d-1)-1$ and $m' \geq 1-(d-1)$. In our three cases above, by Theorem 2.26, $\mathfrak{D}(K) = \mathfrak{D}(K')$, $\mathfrak{D}(K) = v\mathfrak{D}(K')$ or $\mathfrak{D}(K) = v^{-1}\mathfrak{D}(K')$. In the first case, $m = m', M = M'$ and our result holds trivially. The latter cases are similar. In the second case, if $m = m' + 1$ and $M = M' + 1$, we have seen earlier that $M \leq d-1$. If $m' \geq 1-(d-1)$, then $m' + 1 \geq 3-d \geq 1-d$.

– **Inductive case:** $k > 0$. Suppose the result holds for $k' < k$. If b and x_1 do not intersect, then we can view K as a different cascade, one with a changed order \prec in which the ordering merely swaps x_1 and b . Here, the number of intermediate elements in the order is $k-1$ and the result follows from the inductive hypothesis. Otherwise, we must have curves b and x_1 cross. Using regular equivalence, we can move these curves around so they only have one intersection. Take an open ball around only this intersection and create the skein-relation-diagrams from Theorem 2.26 with the typical labels $K = K_+, K_-, K_0, K_\infty$. Observe that K_-, K_0, K_∞ are still cascades. However, K_- can be seen as the modification of K where the linear order swaps the order of curves x_1 and b . Hence, the number of intermediate curves between b and a is smaller so our innermost inductive hypothesis applies. The latter two diagrams have less crossing numbers than K . So if K has the tuple (d, n) as its inductive index, the latter two diagrams have indices $(d, n-1)$. Hence, the outermost inductive hypothesis applies. Write the skein relation:

$$\mathfrak{D}(K_+) = \mathfrak{D}(K_-) + z(\mathfrak{D}(K_0) + \mathfrak{D}(K_\infty))$$

Let m_1, m_2, m_3 and M_1, M_2, M_3 be the minimum and maximum powers of v in the Dubrovnik polynomials of K_-, K_0, K_∞ . Let $m' = \min\{m_i\}$ and $M' = \min\{M_i\}$. By the inductive hypothesis $1-d \leq m'$ and $M' \leq d-1$. From the skein relation, we know $M \leq M'$ and $m' \leq m$. Hence, $1-d \leq m' \leq m$ and $M \leq M' \leq d-1$ as desired.

□

Combining this proof with the previous one we already have a lower bound:

Corollary 4.3 (Morton-Beltrami [6]). *Let D be a regular diagram with grid index $\gamma(D)$. Then,*

$$[\mathfrak{D}_D(v, z)]_v + 2 \leq 2\gamma(D).$$

Proof. Let D be a regular diagram with grid index $\gamma(D)$. By Theorem 4.1, there is a regular diagram D' that is a cascade of degree $\gamma(D)$. Let M and

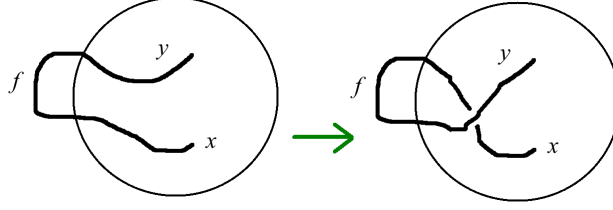


FIGURE 25. Adding curls to a cap f of a cascade with a circular frame.

m be the largest and smallest powers of the Dubrovnik polynomial of D' . By Theorem 4.2,

$$M \leq \gamma(D) - 1 \text{ and } -m \leq \gamma(D) - 1.$$

Adding these inequalities yields $M - m \leq 2\gamma(D) - 2$.

□

4.3. Bounding The Grid Index. With some cleverness, we can use Theorem 4.2 from the previous section to get an even stronger bound on the arc index: Theorem 1.2. This result from [6] states that for any diagram D (or link) $[\mathfrak{D}(D)]_v + 2 \leq \gamma(D)$. We exhibit the proof from [6] with detail.

Proof. Let D be a regular diagram. By Theorem 4.1, we may assume D is a cascade of degree b . Write the Dubrovnik polynomial of D as

$$\mathfrak{D}(D) = \sum_{i=m}^M a_i v^i p_i(z)$$

such that a_m, a_M are nonzero. We want to show $(M - m) + 2 \leq b$. We can achieve this result by modifying D to two new diagrams each of which is also a cascade still of degree b . These diagrams when combined with Theorem 4.2 provide inequalities on m, M which yield the desired result.

Let F be the frame of cascade D with inner region F' . Let (\prec) be the linear order of the cascade D . Construct a new diagram D_{neg} as follows. Let f be any cap of D that connects two curves x, y inside $F' \cap D$ such that when traversing the frame clockwise, we encounter these curves in the order of the smaller then larger curve, i.e., x precedes y where $x \prec y$ on our cap f . See the left of Figure 25.

Make a R_1 move to add a *positive* curl outside the frame and using regular isotopy move it inside the frame as in the right of Figure 25. Change each cap of this form in D this way. Observe that as we do this for each such cap s , we still have a cascade of degree b at the end. Our change for each s introduces exactly one additional crossing between the corresponding curves

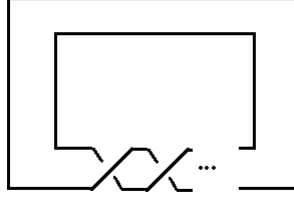


FIGURE 26. A generic twiddle.

x_s and y_s and this crossing respects the linear ordering (\prec), that is, since $x \prec y$, x crosses under y .

Using the curl equations of the Dubrovnik polynomial, we have

$$\mathfrak{D}(D_{neg}) = v^{-l} \mathfrak{D}(D)$$

where l of the b caps of D permit adding a positive curl that respects \prec . Applying Theorem 4.2 to D_{neg} we achieve $m - l \geq 1 - b$.

We can achieve a similar inequality on M . Construct the diagram D_{pos} by taking all the other $b - l$ caps of D and adding a *negative* curl. In those caps if the x curve precedes y curve when moving clockwise around the frame, then $y \prec x$. Now, D_{pos} has Dubrovnik polynomial $\mathfrak{D}(D_{pos}) = v^{b-l} \mathfrak{D}(D)$.

Applying Theorem 4.2 we get $M + (b - l) \leq b - 1$. So, $m - l \geq 1 - b$ which implies $l - m \leq b - 1$. Adding this to $M + (b - l) \leq b - 1$ yields $M + (b - l) + l - m \leq 2b - 2$ which implies $M - m + 2 \leq b$ as desired. \square

5. SHARP BOUND ON TWIST KNOTS

In this section, we show our second lower bound is sharp for a set of knots called twist knots. The work in this section is our own.

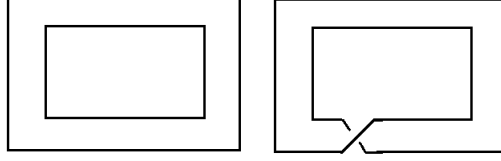
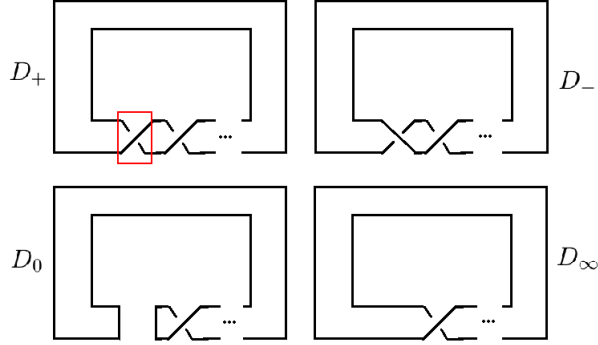
5.1. Twiddles. The bracket polynomial of a twist knot is closely related to the bracket polynomial of a kind of knot that we call a twiddle.

Definition 5.1. A **twiddle** is a knot for which there exists a diagram of the form depicted in Figure 26. We denote such a diagram of a twiddle with $n \geq 0$ positive crossings (depicted using ellipses in the figure) as W_n .

Our goal in this subsection is to establish a few lemmas about the minimum and maximum powers of v in the bracket polynomial of W_n . For this purpose, we introduce some handy notation:

Definition 5.2. We denote by \overline{m}_n and \overline{M}_n the minimum and maximum powers of v of the bracket polynomial of W_n when the polynomial is written in sum of monomial form.

We begin with a calculation on some simple twiddles and move on to a relation on the bracket polynomial of twiddles.

FIGURE 27. Diagrams of W_0 (left) and W_1 (right).FIGURE 28. Calculating the bracket polynomial of W_n for $n > 1$.

Lemma 5.3. *It is the case that $\overline{m_0} = -1$, $\overline{M_0} = 1$ and $\overline{m_1} = \overline{M_1} = 1$.*

Proof. Inspect Figure 27. We can calculate $\mathfrak{D}(W_0)$ by using Proposition 2.29. The diagram W_0 is just the disjoint union of two unknots, i.e., $W_0 = \mathcal{O} \sqcup \mathcal{O}$. Hence,

$$\mathfrak{D}(W_0) = \delta = 1 + z^{-1}(v^{-1} - v).$$

Thus, $\overline{m_0} = -1$, $\overline{M_0} = 1$ and since W_1 is a unknot with a negative curl, $\overline{m_1} = \overline{M_1} = 1$. \square

Lemma 5.4. *For $n > 1$,*

$$\mathfrak{D}(W_n) = \mathfrak{D}(W_{n-2}) + zv^{1-n} - z\mathfrak{D}(W_{n-1}).$$

Proof. Inspect Figure 28 in which $D_+ = W_n$. The crossing in the red box is the one that is changed. We have depicted at least 2 positive crossings because $n > 1$. For the diagram D_- , we can observe that the change we make undoes the crossing to the right of it. That is, we have a twiddle of two less degree (we lost the crossing we manipulated and the undone one), i.e., $D_- = W_{n-2}$. Since we can do this undoing via R_2, R_3 moves (under which \mathfrak{D} does not change), we have $\mathfrak{D}(D_-) = \mathfrak{D}(W_{n-2})$. Now, D_0 is just the unknot with $n-1$ positive curls. So, $\mathfrak{D}(D_0) = v^{-(n-1)} = v^{1-n}$. Finally, D_∞ is simply

W_{n-1} . Using the skein relation $\mathfrak{D}(D_+) - \mathfrak{D}(D_-) = z\mathfrak{D}(D_0) - z\mathfrak{D}(D_\infty)$, we immediately get the desired equality. \square

With this lemma in hand, we can give a general characterization for most $\overline{m_n}$ and $\overline{M_n}$ that we will need later:

Corollary 5.5. *For $n > 1$,*

- (1) $\overline{m_n} = 1 - n$,
- (2) *there is a $(\pm z^{n-1}v)$ term present in $\mathfrak{D}(W_n)$ and there is no $(\pm z^p v)$ term with $p > n - 1$, and*
- (3) $\overline{M_n} = 1$.

Proof. We use induction.

- First, we calculate $\overline{m_n}$ for $n = 2, 3$. For this computation we recall our calculations of $\mathfrak{D}(W_0)$ and $\mathfrak{D}(W_1)$ from Lemma 5.3. From Lemma 5.4, we can compute the following:

$$\begin{aligned}\mathfrak{D}(W_2) &= \mathfrak{D}(W_0) + zv^{-1} - z\mathfrak{D}(W_1) \\ &= (1 + (-v + v^{-1})z^{-1}) + zv^{-1} - zv \\ &= 1 + z^{-1}(-v + v^{-1}) + z(v^{-1} - v)\end{aligned}$$

$$\begin{aligned}\mathfrak{D}(W_3) &= \mathfrak{D}(W_1) + zv^{-2} - z\mathfrak{D}(W_2) \\ &= v + zv^{-2} - z\mathfrak{D}(W_2)\end{aligned}$$

We see $(\overline{m_2}, \overline{M_2}) = (-1, 1)$ as desired. Similarly, we can see $(\overline{m_3}, \overline{M_3}) = (-2, 1)$. We also see a zv term in $\mathfrak{D}(W_1)$ and a z^2v term in $\mathfrak{D}(W_3)$.

- Let $n > 3$. Suppose the inductive hypothesis for $k \leq n$. Write

$$\mathfrak{D}(W_n) = \mathfrak{D}(W_{n-2}) + zv^{1-n} - z\mathfrak{D}(W_{n-1}).$$

- The smallest possible power of v in the $(\mathfrak{D}(W_{n-2}))$ or $(z\mathfrak{D}(W_{n-1}))$ terms are $\overline{m_{n-2}}, \overline{m_{n-1}}$ respectively. By hypotheses, these are $(1 - (n - 2)), (1 - (n - 1))$ and both of these are greater than $(1 - n)$. Hence the term (zv^{1-n}) does not cancel and is a term with the lowest possible power of v . That is, $\overline{m_n} = 1 - n$.
- By the inductive hypothesis, $\mathfrak{D}(W_{n-1})$ has a $z^{n-2}v$ term inside it with no similar term with larger z power. Also, the similar term contained in the first term $(\mathfrak{D}(W_{n-2}))$ with maximal z power is $z^{n-3}v$. Hence, there is a term $z(z^{n-2})v = z^{n-1}v$ which has the highest z power multiplied to v , and so, is not cancelled.

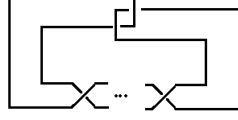


FIGURE 29. A generic twist knot with k positive crossings.

- The largest possible power of v is 1. That is, $\overline{M_n} \leq 1$. By the inductive hypothesis, this applies to both terms $(\mathfrak{D}(W_{n-1}))$ and $(z\mathfrak{D}(W_{n-1}))$. Hence, the largest possible power of v in $\mathfrak{D}(W_n)$ is 1. By part (2) in the statement of this corollary, we are ensured a term with this power. Hence $\overline{M_n} = 1$.

□

5.2. Twist Knots. We can now show that our bracket-based lower bound of the grid index is sharp for a class of knots called twist knots. That is, we prove Theorem 1.3, which states that for a diagram of a twist knot T_n , $[\mathcal{D}(T_n)]_v + 2 = \gamma(T_n)$. Of course, we begin with defining twist knots:

Definition 5.6. **Twist knots** are knots for which there exist diagrams of the form in Figure 29. We denote such a diagram by T_n for $n > 0$ positive crossings.³

As with twiddles, we establish the following useful notation:

Definition 5.7. By m_n and M_n we denote the minimum and maximum powers of v of the bracket polynomial of T_n when the polynomial is written in sum of monomials form.

Our roadmap is to first establish some useful lemmas about m_n and M_n and then use those to calculate the bracket breadth of T_n for $n > 1$. These will allow us to prove Theorem 1.3.

We begin with a useful lemma for calculating m_n and M_n for $n > 0$.

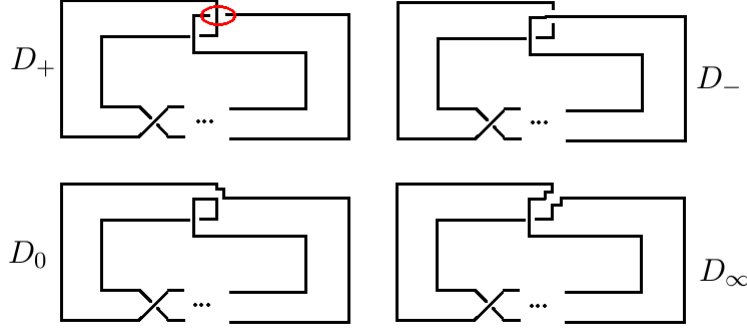
Lemma 5.8. For $n > 0$,

$$\mathfrak{D}(T_n) = v^{-n} + zv^{-1}\mathfrak{D}(W_n) - z\mathfrak{D}(W_{n-1}).$$

Proof. Inspect Figure 30. We form the variations of a generic diagram T_n for $n > 0$. The manipulated crossing is circled red in the original diagram $D_+ = T_n$.

Observe that D_- can be changed via R_2, R_3 moves to just be the unknot with n positive curls. We simply move one of the top loops away from the other. Since the bracket polynomial is invariant over regular moves, we can

³Actually, twist knots can have $n < 0$ positive crossings, that is, $-n$ negative crossings (with the under and over strand reversed), however we do not consider these in this thesis.


 FIGURE 30. Calculating a bracket relation for T_n for $n > 0$.

calculate it over that diagram of n positive curls added to the unknot. This says $\mathfrak{D}(D_-) = v^{-n}$.

When we undo the positive curl at the top of D_0 we get W_n . So, we have $\mathfrak{D}(D_0) = v^{-1}\mathfrak{D}(W_n)$. For D_∞ , our change basically adds a negative crossing. If we slide this along (via R_2, R_3 moves) we undo one crossing in the bottom part of the diagram. This gives us $D_\infty = W_{n-1}$ and since $\mathfrak{D}()$ is invariant under R_2, R_3 moves, $\mathfrak{D}(D_\infty) = \mathfrak{D}(W_{n-1})$.

The equalities $\mathfrak{D}(D_-) = v^{-n}$, $\mathfrak{D}(D_0) = v^{-1}\mathfrak{D}(W_n)$, $\mathfrak{D}(D_\infty) = \mathfrak{D}(W_{n-1})$ and the skein relation $\mathfrak{D}(D_+) - \mathfrak{D}(D_-) = z\mathfrak{D}(D_0) - z\mathfrak{D}(D_\infty)$ give us the desired equality. \square

Finally, as with twiddles, we can get a general characterization for the minimum and maximum powers of v in the bracket polynomial:

Theorem 5.9. *For $n > 1$, $m_n = -n$, $M_n = 1$. Hence, $[\mathfrak{D}(T_n)]_v = n + 1$.*

Proof. We take cases.

- If $n = 2$, we calculate $\mathfrak{D}(T_2)$ using Lemma 5.8:

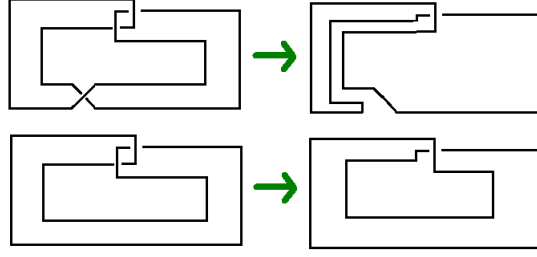
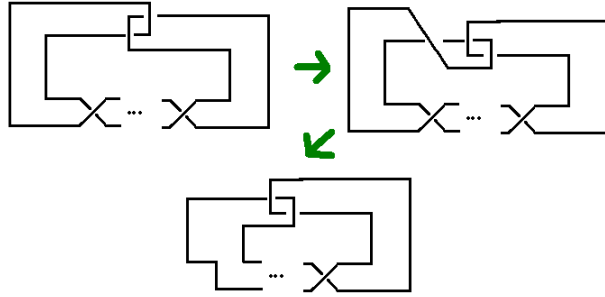
$$\begin{aligned} \mathfrak{D}(T_2) &= v^{-2} + z\mathfrak{D}(W_2) - z\mathfrak{D}(W_1) \\ &= v^{-2} + z\mathfrak{D}(W_2) - zv \end{aligned}$$

Looking at the calculation of $\mathfrak{D}(W_2)$ in Corollary 5.5, we can observe that $(m_2, M_2) = (-2, 1)$ as desired.

- Suppose $n > 2$. Using Lemma 5.8, we write

$$\mathfrak{D}(T_n) = v^{-n} + zv^{-1}\mathfrak{D}(W_n) - z\mathfrak{D}(W_{n-1}).$$

Since $n > 2$, we have $n > 1$ and $n - 1 > 1$. By Corollary 5.5, the smallest power of v in the middle term is one less than $\overline{m}_n = (1 - n)$ and the smallest power of v in the last term is $\overline{m}_{n-1} = (1 - (n - 1))$.

FIGURE 31. Both T_1, T_0 (above, below) are the unknot.FIGURE 32. Changing T_n for $n > 1$ to fit nicely in a grid.

Both of these are larger than $(-n)$ so the (v^{-n}) term does not cancel. Hence, $m_n = -n$.

Also by Corollary 5.5, we know that 1 is largest power of v in both $\mathfrak{D}(W_n)$ and $\mathfrak{D}(W_{n-1})$. Hence, the largest power of v in the middle term $(zv^{-1}\mathfrak{D}(W_n))$ is 0 and in the last term $(-z\mathfrak{D}(W_{n-1}))$ is 1. Since the power of v in the first term is smaller $(-n < 0 < 1)$ than both of these, the term with power 1 in the last term does not cancel. Thus, $M_n = 1$.

□

Finally, we can prove our sharp bound, i.e., Theorem 1.3. That is, if $n \geq 0$, then $[\mathfrak{D}(T_n)]_v + 2 = \gamma(T_n)$.

Proof of Theorem 1.3. We take cases: $n < 2$ and $n \geq 2$.

Look at Figure 31 and observe T_0, T_1 are the unknot. Since the breadth is a knot invariant (and the breadth of the unknot is 0), the breadth of these two knots is 0. Hence, by our bound $0 + 2 \leq \gamma(T_n)$. The unknot can be represented in a 2×2 grid with a square. By definition, $\gamma(T_n) \leq 2$. Hence, for $n < 2$, $\gamma(T_n) = [\mathfrak{D}(T_n)]_v + 2$.

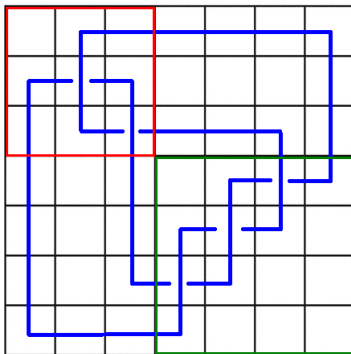


FIGURE 33. An example (for $n = 4$) of diagrams in grid form with grid index $n + 3$ equivalent to T_n for $n > 2$.

Now say $n \geq 2$. By Theorem 5.9 we know that the bracket breadth of T_n is $n + 1$. So, our lower bound is $n + 1 + 2 = n + 3 \leq \gamma(T_n)$.

For such a diagram T_n , make the changes as made in Figure 32. Note that this change decreases the number of crossings at the bottom. Then, we can put such a diagram in grid form as in Figure 33. This figure is an example for $n = 4$. However, to generalize the construction, we simply keep the red box fixed and enlarge the green box as needed. By definition $\gamma(T_n) \leq n + 3$. Hence, $\gamma(T_n) = n + 3$ as desired. \square

REFERENCES

- [1] Colin Conrad Adams. *The knot book: an elementary introduction to the mathematical theory of knots*. American Mathematical Soc., 2004.
- [2] Gerhard Burde, Heiner Zieschang, and Michael Heusener. *Knots*. Vol. 5. Walter de Gruyter, 2013.
- [3] Peter R Cromwell. “Embedding knots and links in an open book I: Basic properties”. In: *Topology and its Applications* 64.1 (1995), pp. 37–58.
- [4] John Franks and RF Williams. “Braids and the Jones polynomial”. In: *Transactions of the American Mathematical Society* 303.1 (1987), pp. 97–108.
- [5] Ciprian Manolescu, Peter Ozsváth, and Sucharit Sarkar. “A combinatorial description of knot Floer homology”. In: *Annals of Mathematics* (2009), pp. 633–660.
- [6] Hugh R Morton and Elisabetta Beltrami. “Arc index and the Kauffman polynomial”. In: *Mathematical Proceedings of the Cambridge Philosophical Society*. Vol. 123. 1. Cambridge University Press. 1998, pp. 41–48.
- [7] Kunio Murasugi. *Knot theory and its applications*. Springer Science & Business Media, 2007.
- [8] Lenhard Ng and Dylan Thurston. “Grid diagrams, braids, and contact geometry”. In: *Proceedings of Gkova Geometry-Topology Conference 2008*. Gkova Geometry/Topology Conference (GGT), Gkova, 2009, 120136.
- [9] Paul M Watkins. *Exploring Knots Through Sculpture*. URL: <https://exploringknots.wordpress.com/page/2/> (visited on 05/03/2019).